

# Risk-based Security Measure Allocation Against Actuator attacks

Sribalaji C. Anand <sup>1</sup> (Student Member, IEEE), André M. H. Teixeira <sup>2</sup> (Member, IEEE)

<sup>1</sup>Department of Electrical Engineering, Uppsala University, PO Box 65, SE-75103, Uppsala, Sweden.

<sup>2</sup>Department of Information Technology, Uppsala University, PO Box 337, SE-75105, Uppsala, Sweden.

CORRESPONDING AUTHOR: Sribalaji C. Anand (e-mail: sribalaji.anand@angstrom.uu.se)

This work is supported by the Swedish Research Council grant 2018-04396 and by the Swedish Foundation for Strategic Research.

**ABSTRACT** This article considers the problem of risk-optimal allocation of security measures when the actuators of an uncertain control system are under attack. We consider an adversary injecting false data into the actuator channels. The attack impact is characterized by the maximum performance loss caused by a stealthy adversary with bounded energy. Since the impact is a random variable, due to system uncertainty, we use Conditional Value-at-Risk (CVaR) to characterize the risk associated with the attack. We then consider the problem of allocating security measures to the set of actuators to minimize the risk. We assume that there are only a limited number of security measures available. Under this constraint, we observe that the allocation problem is a mixed-integer optimization problem. Thus we use relaxation techniques to approximate the security allocation problem into a Semi-Definite Program (SDP). We also compare our allocation method (*i*) across different risk measures: the worst-case measure, the average (nominal) measure, and (*ii*) across different search algorithms: the exhaustive and the greedy search algorithms. We depict the efficacy of our approach through numerical examples.

**INDEX TERMS** Networked control systems, Resilient Control Systems, LMIs, Optimization.

## I. INTRODUCTION

Security of Networked Control Systems (NCSs) has received increased research attention [1], [2]. Following [3], the literature on the security of NCSs can be broadly classified into (i) characterizing the different attack scenarios, (ii) determining the optimal attack strategies and their corresponding impact (performance loss), and (iii) attack mitigation.

In the literature, attack mitigation (defined in [4, Chapter 1]) is performed (mostly) in three methods. The first method is to design mechanisms to detect attacks [5], [6]. The second method is to design the parameters of the closed-loop system (controller gain, for instance) so that the attack impact is minimal [7]–[9]. The third method is to allocate the security measures (encryption for instance) so that the attack impact through the unprotected assets is minimal [10].

### A. Literature review

The problem of security allocation in NCS can be interpreted in different ways. Here we provide three different types of security allocation which can also be found in the literature. Firstly at the device level, consider patching of

Programmable Logic Controllers (PLC) in NCSs. In contrast to classical Information Technology (IT) systems, NCSs have strict real-time requirements which require the operator to carefully consider the risks involved before deploying the security patch [11]. The risk can vary from exposing additional vulnerabilities [12], increasing the downtime, operational costs, etc. Then allocation refers to the problem of deciding which PLCs to be updated with a patch by not enduring a huge performance loss in the presence of attacks.

Secondly, similar to classical IT systems, security allocation can refer to deciding which of the communication channels to encrypt (at the network communication level) [13]. Here, encryption can refer to message authentication or private key encryption which can be implemented in NCS without any significant delays (see [14] and [15]).

Finally, security allocation at the control level refers to choosing the communication channels to add watermarks. There are many strategies in the literature, designed from a control perspective, so that the adversary cannot remain stealthy [16]–[18]. It is to be noted that the allocation of

such control-theoretic strategies for attack detection does not introduce significant delays in the closed-loop system.

The problem of security allocation has been studied extensively in the literature. For instance, the security allocation strategy against sensor attacks in static power systems was investigated in [19]. The work [10] focuses on security allocation for deterministic dynamical systems by exploiting sub-modularity. The optimal sensor/detector placement problem for uncertain systems was studied in [20] using a game-theoretic approach. However, there are three main differences between [20] and our work. Firstly, [20] considers a framework with a single attacked node whereas we consider multiple attacked actuators. Secondly, [20] requires explicitly calculating the game payoff for each pair of players' actions, whereas we propose a single-shot semi-definite program (SDP). Finally, [20] uses the Value-at-Risk (VaR) as the risk metric, whereas we use Conditional VaR (CVaR) as a risk metric, which has much more advantages, notably convexity [21]. We note that game-theoretic approaches have also been used in other research fields not limited to control for optimal allocation of monitoring resources [22], [23]

Other works which focus on optimal security allocation using a game-theoretic approach are [24]–[27]. However, there are three main differences to our approach. Firstly, these works focus on sensor attacks, whereas we focus on actuator attacks. Secondly, these works do not consider uncertain systems but they focus on large-scale systems and their related complexity issues. Finally, these works focus on attack detection only but do not consider the related performance loss caused by attacks. In contrast, we consider a metric that takes into account the performance loss as well as the detection performance; see [28] and [4, Chapter 4]. One of our previous works [29] also uses a similar metric for optimizing CVaR, however, it focuses on controller design rather than security allocation. Finally, another of our previous works [30] focuses on allocation for uncertain systems. However, [30] is based on an exhaustive search.

### B. Problem setup

As mentioned in the literature study, the allocation problem for uncertain systems has not been studied yet. Nonetheless, uncertainties are inevitable in physics-based [31] or data-based modeling techniques [32]. To address this gap, we consider an uncertain linear time-invariant process (1). Since the process is controlled with a feedback controller (2) over a wireless network, it is prone to cyber-attacks. Thus, we consider false data injection attacks on the actuators and an observer-based detector (3). The closed loop system under attack is described in (1)–(3) (also see Figure 1)

$$\mathcal{P} : \begin{cases} \dot{\hat{x}}(t) &= A^\Delta \hat{x}(t) + B^\Delta \tilde{u}(t) \\ y(t) &= C\hat{x}(t) \\ y_p(t) &= C_j \hat{x}(t) \end{cases} \quad (1)$$

$$\mathcal{C} : \begin{cases} \dot{z}(t) &= A_c z(t) + B_c y(t) \\ u(t) &= C_c z(t) + D_c y(t) \end{cases} \quad (2)$$

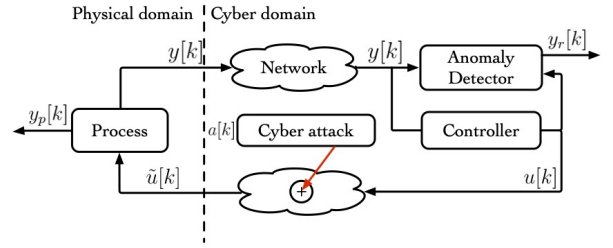


FIGURE 1. NCS under false data injection attack on actuators

$$\mathcal{D} : \begin{cases} \dot{\hat{x}}_p(t) &= A\hat{x}_p(t) + Bu(t) + Ky_r(t) \\ y_r(t) &= y(t) - C\hat{x}(t) \end{cases} \quad (3)$$

where  $A^\Delta \triangleq A + \Delta A(\delta)$  with  $A$  representing the nominal system matrix, and the parametric uncertainty characterized by  $\Delta A(\delta)$ ,  $\delta \in \Omega$ . We assume  $\Omega$  to be closed, bounded, and to include the zero uncertainty yielding  $\Delta A(0) = 0$ . The other matrices are similarly expressed. The state of the process, controller, and detector is represented by  $\bar{x}(t) \in \mathbb{R}^{n_x}$ ,  $z(t) \in \mathbb{R}^{n_z}$  and  $\hat{x}_p(t) \in \mathbb{R}^{n_x}$  respectively. The control signal generated by the controller and the control signal received by the process is  $u(t) \in \mathbb{R}^{n_u}$  and  $\tilde{u}(t) \in \mathbb{R}^{n_u}$  respectively. The measurement output, performance output, and residue output are denoted by  $y(t) \in \mathbb{R}^{n_m}$ ,  $y_p(t) \in \mathbb{R}^{n_p}$  and  $y_r(t) \in \mathbb{R}^{n_m}$  respectively.

We consider an adversary with complete system knowledge injecting false data into the actuator channel. The operator is the only one with uncertainties in system knowledge. This setup might be unrealistic, but it helps us study the worst-case scenario. The main problem investigated in this article is formulated next.

**Problem 1.** *Given the uncertain NCS is under attack, and that we can secure a small number of actuators ( $n_w$ ), how to optimally allocate the security measures?*  $\triangleleft$

### C. Contributions

To the best of the authors' knowledge, the problem of security allocation for uncertain systems using CVaR has not been addressed in the literature. To this end, the main contributions of the article are as follows

- 1) We formulate the optimal allocation problem for uncertain systems using CVaR as a risk metric. The attack impact is characterized by the maximum performance loss caused by a stealthy adversary with limited energy.
- 2) The impact metric is non-convex in the design variable. Hence we derive a convex *impact proxy* which also serves as the upper bound for the impact.
- 3) The allocation problem using CVaR and the proposed impact proxy is a mixed integer SDP which is generally hard to solve [33]. Through relaxations, we propose an approximate SDP to solve the allocation problem, along with posterior guarantees on the optimality gap.
- 4) We compare our solution across different risk measures (worst-case, and nominal measures) and different search algorithms (exhaustive, and greedy search).

The rest of this article is organized as follows: We formulate the problem in Section II. We propose a convex SDP to solve Problem 1 approximately in Section III. We outline the solution to the security allocation problem under different risk measures in Section IV. We describe the exhaustive search algorithm and greedy search algorithm in Section V, where we also compare the methods briefly. We depict the efficacy of our proposed approach through numerical examples in Section VI and conclude in Section VII.

#### D. Notation

A positive (semi-) definite matrix  $A$  is denoted by  $A \succ 0$  ( $A \succeq 0$ ). Let  $x : \mathbb{R} \rightarrow \mathbb{R}^n$  be a continuous-time signal with  $x(t)$  as the value of the signal  $x$  at the time  $t$ . Let the time horizon be  $[0, N] = \{t \in \mathbb{R}^+ \mid 0 \leq t \leq N\}$ . The  $\mathcal{L}_2$ -norm of  $x$  over the horizon  $(0, N)$  is represented as  $\|x\|_{\mathcal{L}_2, (0, N)}^2 \triangleq \int_{t=0}^N x(t)^T x(t)$ . Let the space of square integrable signals be defined as  $\mathcal{L}_2 \triangleq \{x : \mathbb{R}^+ \rightarrow \mathbb{R}^n \mid \|x\|_{\mathcal{L}_2, (0, \infty)}^2 < \infty\}$  and the extended signal space be defined as  $\mathcal{L}_{2e} \triangleq \{x : \mathbb{R}^+ \rightarrow \mathbb{R}^n \mid \|x\|_{\mathcal{L}_2, (0, N)}^2 < \infty, \forall N \in \mathbb{R}^+\}$ . For the sake of simplicity, we represent  $\|x\|_{\mathcal{L}_2, (0, \infty)}^2$  as  $\|x\|_{\mathcal{L}_2}^2$ . Given a vector  $f \in \mathbb{R}^N$ , let  $\{x_i\}$  be the  $N$  indices of entries of  $f$  such that  $f(x_1) \geq f(x_2) \geq \dots \geq f(x_N)$ . Then, the  $(N - i + 1)$ -th order statistic of  $f$  is given by  $f(x_i)$ . And  $f^{[j]}$ ,  $j \leq N$  represents the  $j$ -th element of the vector  $f$ .

## II. Problem Formulation

The system (1)-(3) is said to have a good performance when  $\|y_p\|_{\mathcal{L}_2}^2$  is small. This is similar to linear quadratic (LQ) control where the objective is to minimize performance loss. Similarly, an anomaly is considered to be detected when the detector output energy  $\|y_r\|_{\mathcal{L}_2}^2$  is greater than a predefined threshold, say  $\epsilon_r$ . Given this setup, we next describe the adversary in detail and later formulate the problem.

#### A. Disruption and disclosure resources

The adversary can access (eavesdrop) the control channels and can inject data. This is represented by

$$\tilde{u}(t) \triangleq u(t) + B_a a(t)$$

where  $a(t) \in \mathbb{R}^{n_u}$  is the data injected by the adversary. The matrix  $B_a$  is a diagonal matrix with  $B_a(i, i) = 1$  if the actuator channel  $i$  is under attack and zero otherwise. The matrix  $B_a$  is square, however, this does not enforce the adversary to attack all the actuators. If the adversary is interested in attacking some of the actuators, the adversary can simply set the corresponding attack vector to zero.

In general,  $B_a$  is chosen by the operator for analysis purposes. If the operator believes that the actuator channel (say  $j$ ) might be under attack, then the corresponding channel has an entry 1 ( $B_a(j, j) = 1$ ). In the rest of the article, the matrix  $B_a$  is called the *attack matrix*.

#### B. Attack goals and constraints.

The adversary's objectives are contrary to that of the operator. That is, the adversary aims to disrupt the system's

behavior while staying stealthy. The system disruption is evaluated by the increase in energy of the performance output, whereas the adversary is stealthy if the energy of the detection output is below a predefined threshold (namely  $\epsilon_r$ ).

In reality, the adversary stops attacking the system after some unknown time  $T < \infty$ . Additionally, the corrupted input signal is applied by physical actuators which have actuator bounds. Thus we consider the energy of the attack signal to be bounded by a predefined threshold (namely  $\epsilon_a$ ).

#### C. System knowledge

Next, we consider that the adversary has full system knowledge, i.e., s/he knows the system matrices (1)-(3). We define such an adversary as an omniscient adversary.

**Definition II.1** (Omniscient adversary). *An adversary is defined to be omniscient if it knows the matrices in (4).*  $\triangleleft$

In reality, it is hard to know the system matrices of (4) due to uncertainty. Thus, such an adversarial setup is far from reality but can help study the worst case. Readers interested in realistic setups where the adversary also has uncertainty are referred to [34]. However, as mentioned in [34], analysis of such realistic setups is computationally intensive. Thus, in this article, we focus on the omniscient adversary.

Defining  $x(t) \triangleq [x_p(t)^T \ z(t)^T \ \hat{x}_p(t)^T]^T$ , the closed-loop system under attack with the performance output and detection output as system outputs becomes

$$\begin{aligned} \dot{x}(t) &= A_{cl}^\Delta x(t) + B_{cl}^\Delta a(t), \\ y_p(t) &= C_p x(t), \\ y_r(t) &= C_r x(t), \end{aligned} \quad (4)$$

with  $\begin{bmatrix} A_{cl}^\Delta & B_{cl}^\Delta \end{bmatrix} =$

$$\begin{bmatrix} A^\Delta + B^\Delta D_c C & B^\Delta C_c & 0 & B^\Delta B_a \\ B_c C & A_c & 0 & 0 \\ (B D_c + K_e) C & B C_c & A - K C & 0 \end{bmatrix}$$

$C_p \triangleq [C_j \ 0 \ 0]$ , and  $C_r \triangleq [C \ 0 \ -C]$ .

In (4), the signals  $x$ ,  $y_p$ , and  $y_r$  are also functions of uncertainty, and the superscripts are dropped for simplicity. Next, we establish the following assumptions.

**Assumption II.1.** *Closed-loop system (4) is stable  $\forall \delta \in \Omega$ .*  $\triangleleft$

**Assumption II.2.** *The tuple  $(A_{cl}^\Delta, B_{cl}^\Delta)$  is controllable  $\forall \delta \in \Omega$ . The tuple  $(A_{cl}^\Delta, [C_p^T \ C_r^T]^T)$  is observable  $\forall \delta \in \Omega$ .*  $\triangleleft$

Assumption II.1 states that the feedback controller robustly stabilizes the plant. Assumption II.2 is a direct consequence (and a common assumption in dissipative systems theory) of [35] which is later used to formulate the proof of Lemma III.2. We later also briefly discuss the consequence of relaxing Assumption II.2 (See Remark 4).

#### D. Optimal allocation problem

Consider the data injection attack scenario where the parametric uncertainty  $\delta \in \Omega$  of the system is known to the adversary but not to the defender. Under this setup, the

adversary can cause high disruption by remaining stealthy as it will be able to inject attacks by solving (5),

$$q(B_a, \delta) \triangleq \sup_{a \in \mathcal{L}_{2e}} \|y_p[B_a, \delta]\|_{\mathcal{L}_2}^2 \quad (5)$$

$$\text{s.t. } \|y_r[B_a, \delta]\|_{\mathcal{L}_2}^2 \leq \epsilon_r$$

$$\|a[\delta]\|_{\mathcal{L}_2}^2 \leq \epsilon_a, \quad x[B_a, \delta](0) = 0,$$

where  $y_p[B_a, \delta]$ ,  $y_r[B_a, \delta]$ , and  $a[\delta]$  are the performance output, detection output, and the attack vector corresponding to the matrix  $B_a$  and uncertainty  $\delta$ , and  $q(\cdot)$  is the impact caused by the adversary on (4). Such a setup in (5) is considered for the adversary, to analyze the worst-case impact of stealthy attacks, since the adversary will be able to inject undetectable attacks which cause high performance deterioration. For the defender,  $q(B_a, \delta)$  becomes a random variable since  $\delta$  is unknown. The defender only knows the bounds of the set  $\Omega$ , the nominal system matrices in (4).

Thus, the defender protects some of the actuators (through encryption for example) such that the risk corresponding to  $q(\cdot)$  in (5) is minimized. However, the defender also has the constraint that there are only a limited number of security measures i.e.,  $n_w < n_u$  (C1). Recall that the diagonal entries of the matrix  $B_a$  can either be 1 (unprotected) or 0 (protected) (C2). Then *Problem 1* can be re-formulated as

**Problem 2.** Find the optimal diagonal matrix  $B_a^*$  such that

$$B_a^* \triangleq \arg \inf_{B_a} \mathcal{R}_\Omega(q(B_a, \delta))$$

$$\text{s.t. } \sum_{i=1}^{n_u} B_a(i, i) \geq n_u - n_w, \quad (C1) \quad (6)$$

$$B_a(i, i) = \{0, 1\} \quad (C2)$$

where  $\mathcal{R}_\Omega$  is a risk metric chosen by the defender. The subscript  $\Omega$  denotes that the risk acts over the set  $\Omega$  whose probabilistic description is known to the defender (for the results of this article to hold, it is sufficient that the defender can draw samples from the set  $\Omega$ ).  $\triangleleft$

CVaR is extensively used in the literature due to its numerous advantages [21]. Thus we choose the CVaR as a risk metric in *Problem 2*. Before we introduce the risk metric, we make the following assumptions that follow from [21].

**Assumption II.3.** The defender can draw samples from the set  $\Omega$  and the function  $q(\cdot, \delta)$  is continuous.  $\triangleleft$

**Definition II.2.** Given a random variable  $q(\cdot, \delta)$  with density  $p(q)$ , the  $\text{CVaR}_\alpha(q(\cdot, \delta))$  (given  $\alpha \in (0, 1)$ ) is given by

$$\frac{1}{1 - \alpha} \int_{q(\cdot, \delta) | q(\cdot, \delta) \geq \text{VaR}_\alpha\{q(\cdot, \delta)\}} q(\cdot, \delta) p(q) dq$$

where  $\text{VaR}_\alpha\{q(\cdot, \delta)\} \triangleq \inf\{x | \mathbb{P}_\Omega[q(\cdot, \delta) \leq x] \geq 1 - \alpha\}$   $\triangleleft$

Next, we illustrate the risk metrics through an example, whereby also motivating the choice of the risk metric.

**Example II.1.** Consider the system in (1)-(3) where

$$[A^\Delta \mid C^T] = \begin{bmatrix} -1 & 0 & 0 & \delta & | & 1 \\ 1 & -5 & 0 & 0 & | & 0 \\ 1 & 1 & -9 & 0 & | & 1 \\ 10 & 1 & 10 & -1 & | & 0 \end{bmatrix} \quad (7)$$

$$\begin{bmatrix} -L \\ K \\ C_j \end{bmatrix} = \begin{bmatrix} 5.26 & 0.44 & 1.64 & 1.99 \\ 0.44 & 0.13 & 0.14 & 0.17 \\ 1.64 & 0.14 & 0.61 & 0.68 \\ 1.99 & 0.17 & 0.68 & 0.87 \\ \hline 5.70 & 0.70 & 0.55 & 15.28 \\ \hline 1 & 1 & 1 & 1 \end{bmatrix},$$

$\delta \in \Omega \triangleq [0, 3]$ , and  $B = C_j^T$ . We set  $\epsilon_r = 1$ , and  $\epsilon_a = 300$ . We determine the value of the random variable  $q(\cdot, \delta)$  in (5) for different uncertainty realizations  $\delta \in \Omega$  and plot the probability density function of  $q(\cdot)$  in Figure 2. We depict the value of the risk measures:  $\text{VaR}_{0.1}\{q(\cdot)\}$ ,  $\text{CVaR}_{0.1}\{q(\cdot)\}$ ,  $\mathbb{E}\{q(\cdot)\}$ , worst-case (similar to  $H_\infty$  control [36]), and nominal measure (without considering uncertainties). Detailed definitions of worst-case and nominal measures are given in Section IV.A and IV.B respectively.

Let  $x = \text{VaR}_\alpha\{q(\cdot)\}$ . Then by optimizing the VaR, one optimizes the probability that the value of  $q(\cdot) \geq x$ . However, VaR does not take into account the thickness of the tail pdf of  $q(\cdot)$ . In general, although we want the risk of attacks to be minimal, we allow for events whose probability is very low but with a high impact. In such scenarios, optimizing the worse case measure might be conservative. The nominal measure is also conservative since it does not consider uncertainties. Given the above arguments, we choose CVaR as the risk metric in this article.  $\triangleleft$

In our setting, the defender determines the attack matrix  $B_a$  such that  $\text{CVaR}_\alpha q(B_a, \delta)$  (given  $\alpha$ ) is minimized. To this end, *Problem 2* can be reformulated as

$$B_a^* = \arg \inf_{B_a} \left\{ \text{CVaR}_\alpha\{q(B_a, \delta)\} \mid (C1), (C2) \right\}. \quad (8)$$

Although CVaR is a convex function, there are three difficulties in solving (8). Firstly,  $q(\cdot)$  is non-convex in the design variable  $B_a$ , which we address in Section III.A. Secondly, the design variable  $B_a$  is binary (C2) which makes the design problem non-convex, and we address this issue in Section III.B. Finally, CVaR cannot be efficiently evaluated exactly since  $\Omega$  is continuous. We describe an empirical approach to solve (8) in Section III.C. Before we discuss the solution to (8), we briefly discuss the relation between (5) and other attack impact metrics in the literature.

**Remark 1** (Relation between Problem 2 and a Stackelberg game). *Problem 2* can be related to a Stackelberg game [24] as follows. The defender first selects the action ( $B_a$ ), i.e., which actuators to protect. Then, the adversary selects the attack ( $a \in \ell_{2e}$ ) through the unprotected actuators and computes the optimal attack by solving (5). Thus *Problem 2* can also be viewed from a game theoretic point of view.  $\triangleleft$

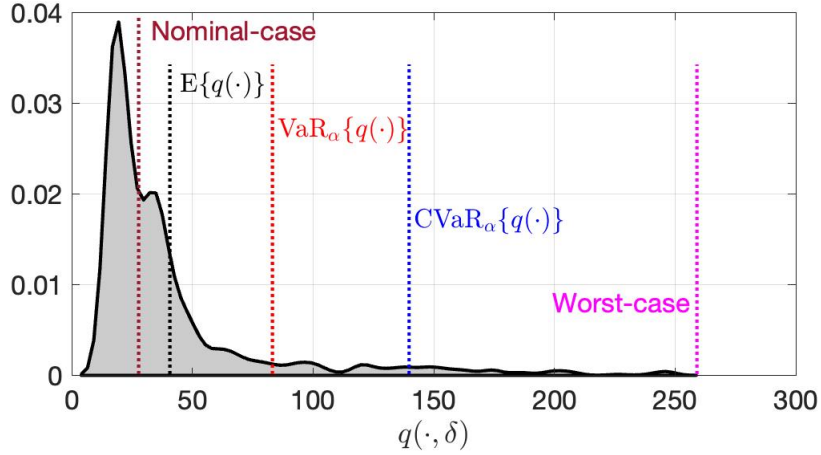


FIGURE 2. Probability distribution function of the random variable  $q(\cdot, \delta)$  and the corresponding risk measures.

**Remark 2** (Boundedness of risk metric). *The concept of risk is sensible when it is finite. In our setup, the risk is finite if the random variable  $q(\cdot)$  is finite. Thus, in the rest of the sequel, we assume that  $q(\cdot, \delta)$  is bounded  $\forall \delta \in \Omega$ . Since the closed loop system is stable, the value of  $q(\cdot, \delta)$  in (5) is unbounded iff  $\|y_p[\cdot, \delta]\|_{\mathcal{L}_2}^2$  is unbounded, which consequently is unbounded iff  $\|a[\delta]\|_{\mathcal{L}_2}^2$  is unbounded. But we know that  $\|a[\delta]\|_{\mathcal{L}_2}^2 \leq \epsilon_a$  where  $\epsilon_a$  is bounded. Thus the assumption on the boundedness of the random variable  $q(\cdot)$  is logical.* ◁

**Remark 3.** *When  $\alpha \rightarrow 1$ , the optimization problem (8) minimizes the worst case impact (5) across all uncertainties. However, as explained in Example II.1 and [37], such approaches can be conservative.* ◁

### E. Relation between (5) and other metrics

In this article, for any given uncertainty  $\delta \in \Omega$ , we use (5) to capture the amount of disruption caused by the adversary. However, other security metrics in the literature can be related to the metric (5).

Let  $\epsilon_r \gg \epsilon_a$ . That is, the detection threshold becomes very large that the constraint on the detection output becomes inactive. Then (5) becomes the  $H_\infty$  metric where the attack is treated as the disturbance. An SDP to determine the  $H_\infty$  metric can be found in [38, (6)]. Works such as [39], [40] for instance, use the  $H_\infty$  metric for measuring attack impact.

On the other hand, when  $\epsilon_a \gg \epsilon_r$ , the constraint on the attack energy becomes inactive. Then (5) is the Output-to-Output Gain (OOG) [4, Chapter 6]. OOG has many advantages over the  $H_\infty$  and  $H_-$  metric which we discussed in [28]. An SDP to determine the OOG can be found in [4, (6.18)]. We combine the above results in Proposition II.1.

**Proposition II.1.** *Consider the CT system under attack described in (4) and the corresponding impact metric described in (5). Then, given  $\delta \in \Omega$ , the following statements are true.*

- 1) *Let  $\epsilon_a$  be a constant, and let  $\gamma_a$  represent the classical  $H_\infty$  gain of the closed loop system (4) for a given  $\delta \in \Omega$ . Then it holds that  $\lim_{\epsilon_r \rightarrow \infty} q(B_a, \delta) = \gamma_a \epsilon_a$ .*

- 2) *Let  $\epsilon_r$  be a constant, and let  $\gamma_r$  represent the OOG [4, (6.18)] of closed-loop system (4) for a given  $\delta \in \Omega$ . Then it holds that  $\lim_{\epsilon_a \rightarrow \infty} q(B_a, \delta) = \gamma_r \epsilon_r$ .* ◻

The objective of the exercise in Proposition II.1 is to show that the allocation results in this article, which are based on the metric (5), can be related to other results (based on  $H_\infty$  metric or OOG) by varying the value of  $\epsilon_r$  and  $\epsilon_a$ . In the next section, we start to solve (8).

## III. Convex SDP for optimal allocation

In this section, we first consider a sampled uncertainty  $\delta_i$  and show that, given  $B_a$ , the value of  $q(B_a, \delta_i)$  can be determined via a convex SDP. We also show that the SDP is a non-convex function of the design variable  $B_a$ . Then we propose a relaxed SDP which is convex in  $B_a$ . We later use this relaxed SDP, to formulate a convex allocation problem.

### A. Convex relaxation for the impact metric

Let us consider the impact metric  $q(B_a, \delta_i)$  in (5). We show in Lemma III.1 that its value can be determined by its convex dual (the proof of Lemma III.1 and all the other results in the sequel are presented in the Appendix).

**Lemma III.1.** *Given a sampled uncertainty  $\delta_i$ , and an attack matrix  $B_a$ , the value of the impact  $q(B_a, \delta_i)$  can be calculated by its convex dual counterpart (9) where  $\gamma_1$  and  $\gamma_2$  are the Lagrange multipliers of the constraints.*

$$\begin{aligned} & \inf_{\gamma_1, i, \gamma_2, i} \quad \epsilon_r \gamma_{1, i} + \epsilon_a \gamma_{2, i} \\ & \text{s.t.} \quad \|y_p[B_a, \delta_i]\|_{\mathcal{L}_2}^2 - \gamma_1 \|y_r[B_a, \delta_i]\|_{\mathcal{L}_2}^2 \\ & \quad \quad - \gamma_2 \|a[\delta_i]\|_{\mathcal{L}_2}^2 \leq 0, \forall a \in \mathcal{L}_{2e} \quad (9) \\ & \quad \quad x[B_a, \delta_i](0) = 0, \gamma_{1, i} \geq 0, \gamma_{2, i} \geq 0. \end{aligned}$$

Although (9) is convex, it is hard to solve (9) since the constraints lie in the signal space. Thus, we use dissipative system theory to re-write (9) as a convex SDP.

Before we formulate this SDP, we introduce the following notation. The matrices in (4) under a sampled uncertainty  $\delta_i$  is denoted as  $A_{cl, i}$ ,  $B_{cl, i}$ ,  $C_p$  and  $C_r$ . Correspondingly the

signals under the sampled uncertainty  $\delta_i$  becomes  $a_i, y_{p,i}, y_{r,i}$  and  $x_i$ . We also know from (4) that  $B_{cl,i}^T$  takes the form  $[B_a^T B_i^T \ 0 \ 0]$  and thus is a linear function in  $B_a$ .

**Lemma III.2.** *Let Assumption II.2 hold. Then, for a sampled uncertainty  $\delta_i$ , the optimization problems (9) and (10) are equivalent.*

$$\begin{aligned} \min_{\mathcal{S}_1} \quad & \epsilon_r \gamma_{1,i} + \epsilon_a \gamma_{2,i} \\ \text{s.t.} \quad & \begin{bmatrix} \mathcal{W}_i & P_i B_{cl,i} \\ B_{cl,i}^T P_i & -\gamma_{2,i} I \end{bmatrix} \preceq 0 \quad (C3_i) \end{aligned} \quad (10)$$

where  $\mathcal{S}_1 \triangleq \{P_i \succ 0, \gamma_{1,i} \geq 0, \gamma_{2,i} \geq 0\}$ , and  $\mathcal{W}_i = A_{cl,i}^T P_i + P_i A_{cl,i} + C_p^T C_p - \gamma_{1,i} C_r^T C_r$ .  $\square$

Lemma III.2 proposes an SDP to determine  $q(\cdot)$  under a sampled uncertainty. However, (10) is non-convex in  $B_a$  as (C3<sub>i</sub>) contains the term  $P_i B_{cl,i}$  which is bi-linear (since  $B_{cl,i}$  is a linear function of  $B_a$ ). Thus, we propose a relaxed SDP in place of (10) which is convex in  $B_a$ . Henceforth, the value of this relaxed SDP is denoted by  $\tilde{q}(\cdot)$ .

The main objective of proposing this relaxed SDP is: once we show that  $\tilde{q}(\cdot)$  is a convex function of the design variable  $B_a$ , we can substitute this convex function  $\tilde{q}(\cdot)$  into the definition of CVaR in (8) (replacing the non-convex function  $q(\cdot)$ ) and optimize it. Now we state our main result.

**Theorem III.3.** *Given a sampled uncertainty  $\delta_i$ , the SDP*

$$\begin{aligned} \min_{\mathcal{S}_2} \quad & \epsilon_r \gamma_{1,i} + \epsilon_a \gamma_{2,i} \\ \text{s.t.} \quad & \begin{bmatrix} -I & 0 & C_p X_i & 0 \\ 0 & -\gamma_{1,i} I & I & 0 \\ X_i C_p^T & I & \mathcal{W}_{2,i} & B_{cl,i} \\ 0 & 0 & B_{cl,i}^T & -\gamma_{2,i} I \end{bmatrix} \preceq 0 \quad (C4) \quad (11) \\ & \mathcal{S}_2 = \{X_i \succ 0, \gamma_{1,i} \geq 0, \gamma_{2,i} \geq 0\}, \end{aligned}$$

whose optimal value is denoted by  $\tilde{q}(\cdot)$ , is a convex relaxation of (10). In the optimization problem (11),  $\mathcal{W}_{2,i} = X_i A_{cl,i}^T + A_{cl,i} X_i - X_i U^T - U X_i$ ,  $\mathcal{S}_2 \triangleq \{X_i, \gamma_{1,i}, \gamma_{2,i}\}$  and  $U \in \mathbb{R}^{2n_x \times 2n_x}$  is given by the Cholesky decomposition:  $C_r^T C_r = U^T U$ .  $\square$

In Theorem III.3, we proposed a convex relaxation of (10), which is non-convex in the design variable  $B_a$ . Next, we show that for a given  $\delta_i$ , the value of the relaxed problem (11) serves as an upper bound to the value of (10).

**Lemma III.4.** *Let the optimal tuple of (11) be represented by  $(\bar{X}_i, \bar{\gamma}_{1,i}, \bar{\gamma}_{2,i})$ . Then the tuple  $(\bar{P}_i \triangleq \bar{X}_i^{-1}, \bar{\gamma}_{1,i}, \bar{\gamma}_{2,i})$  is a feasible solution to the optimization problem (10). Consequently, the optimal value of (11) is greater than or equal to the optimal value of (10).*  $\square$

In this section, we proposed an SDP, convex in  $B_a$  to determine the upper bound  $\tilde{q}(B_a, \delta_i)$  for any given  $B_a$  and sampled uncertainty  $\delta_i$ . The upper bound  $\tilde{q}(\cdot)$  can act as a proxy for the impact  $q(\cdot)$  and provide a certificate of the magnitude of the impact. In the next section, we relax the non-convex constraint (C2)

**Remark 4.** *Assumption II.2 is necessary to prove Lemma III.2 using dissipative system theory (DST). When this assumption fails, there exists a sub-space of the closed-loop system that is uncontrollable/observable (UCO). For the exact treatment of such systems, the UCO subspace should be removed from the closed-loop system dynamics before formulating the Matrix Inequalities (MI) in (10) using DST. However, if the closed-loop system is non-minimal, the MI in (9) are only sufficient conditions for the constraints of (9) to hold. Thus, when assumption (II.2) fails, (10) represents an upper bound on the value of (9).*  $\triangleleft$

## B. SDP relaxation of binary constraint

Using the results of the previous section, to avoid the non-convex relation between  $q(\cdot)$  and  $B_a$  in (8), we replace  $q(\cdot)$  by  $\tilde{q}(\cdot)$  in (8) and formulate (12).

$$\inf_{B_a} \left\{ \text{CVaR}\{\tilde{q}(B_a, \delta)\} \mid (C1), (C2) \right\}. \quad (12)$$

The optimization problem (12) is non-convex since it involves SDP constraints with binary variables (C2). As a first step toward relaxing (C2), we reformulate (12) next.

**Lemma III.5.** *The optimization problems (12) and (13) are equivalent.*

$$\begin{aligned} \inf_{Z, z \in \mathbb{R}^{n_u}} \quad & \text{CVaR}\{\tilde{q}(\text{diag}(z), \delta)\}. \\ \text{s.t.} \quad & \begin{bmatrix} Z & z \\ z^T & 1 \end{bmatrix} \succ 0, \sum_{i=1}^{n_u} z_i \geq n_u - n_w, \quad (C10) \quad (13) \\ & \text{diag}(Z) = z, \text{rank}(Z) = 1. \end{aligned}$$

In Lemma III.5, we reformulated (12) with binary constraints as (13). However, this reformulation has rank constraints due to which (13) is still non-convex. To make the design problem convex, we remove the rank constraint.

**Corollary III.5.1.** *A convex relaxation of (13) is given by*

$$\inf_{Z, z} \left\{ \text{CVaR}\{\tilde{q}(\text{diag}(z), \delta)\} \mid (C10), \text{diag}(Z) = z \right\} \quad (14)$$

Corollary III.5.1 provides a method to relax (C2) as an LMI constraint. There are many approaches in the literature to relax a binary variable constraint [41, Table 1]. However, we chose an LMI relaxation due to its simplicity.

The result  $z$  from (14) will be integer instead of binary-valued. However, from Lemma III.5, we know that if the optimal  $Z$  from (14) has rank 1, then the solution of (14) is equal to the solution of (13), and will be binary. For the general case, when the rank constraint is not satisfied, we provide a heuristic to convert the integers to binary variables later [42]. Next, we approximate the risk metric empirically.

## C. Empirical approximation of CVaR

The optimization problem (14) is hard to solve since the CVaR operates over the set  $\Omega$  which is a continuum (a similar observation was made in [37]). However, when we replace the uncertainty set  $\Omega$  with, a sampled set with  $N$  samples, the CVaR can be approximated by [21, (9)]

$$\begin{aligned}
\min_{S_5} \quad & v + \frac{1}{N(1-\alpha)} \sum_{i=1}^N t_i \\
\text{s.t.} \quad & \begin{bmatrix} -I & 0 & C_p X_i & 0 \\ 0 & -\gamma_{1,i} I & I & 0 \\ X_i C_p^T & I & W_{2,i} & B_{cl,i}(z) \\ 0 & 0 & B_{cl,i}(z)^T & -\gamma_{2,i} I \end{bmatrix} \preceq 0 \quad \forall i \in \Omega_N \quad (C5) \\
& t_i \geq \epsilon_r \gamma_{1,i} + \epsilon_a \gamma_{2,i} - v, \quad \forall i \in \Omega_N \quad (C6) \\
& t_i \geq 0, \quad \forall i \in \Omega_N \quad (C7) \\
& X_i \succ 0, \quad \forall i \in \Omega_N \quad (C8) \\
& \gamma_{1,i} \geq 0, \gamma_{2,i} \geq 0, \quad \forall i \in \Omega_N \quad (C9) \\
& \begin{bmatrix} Z & z \\ z^T & 1 \end{bmatrix} \succeq 0, \quad n_u - n_w \leq \sum_{i=1}^{n_u} z_i \quad (C10) \\
& S_5 \triangleq \{z, Z\} \cup \{\cup_{i=1}^N \{t_i, X_i, \gamma_{1,i}, \gamma_{2,i}\}\} \\
& B_a = \text{diag}(z), \quad \text{diag}(Z) = z, \quad \Omega_N = \{1, \dots, N\}.
\end{aligned} \tag{15}$$

$$\text{CVaR}_\alpha \{\tilde{q}(\cdot, \delta)\} \approx \inf_v v + \frac{1}{1-\alpha} \frac{1}{N} \sum_{i=1}^N [\tilde{q}(\cdot, \delta_i) - v]^+, \tag{16}$$

where given  $X \in \mathbb{R}, [X]^+ \triangleq \max\{X, 0\}$ . Thus using (16), (14) can be written as

$$\inf_{z, Z} \left\{ v + \frac{1}{N(1-\alpha)} \sum_{i=1}^N [\tilde{q}(\cdot) - v]^+ \mid \begin{array}{l} (C10), \\ \text{diag}(Z) = z \end{array} \right\} \tag{17}$$

Now we briefly comment on the convergence of the empirical CVaR (17) to the true CVaR (14). However, the proof of the following lemma is omitted as it is similar to the proof of [43, Theorem 6].

**Lemma III.6.** *Let  $\alpha$  represent the risk threshold. Given  $N$  and  $\alpha$ , let  $\tilde{r}_N$  represent the optimal value of (17), and let  $\tilde{r}$  represent the optimal value of (14). Then it holds that  $\lim_{N \rightarrow \infty} \tilde{r}_N \rightarrow \tilde{r}$ .  $\square$*

Lemma III.6 states that the empirical CVaR almost surely converges to the true CVaR in the large sample case. Now, we present a convex SDP to solve (17) in Lemma III.7.

**Lemma III.7.** *Let us represent the optimal value of (15) as  $\gamma$ , and the optimal argument of  $z \in \mathbb{R}^{n_u}$  from (15) as  $\underline{z}$ . Then an approximate binary solution to (17) is given by*

$$\bar{B}_a(i, i) = \begin{cases} 0, & \text{if } \underline{z}_i \text{ belongs to statistics of} \\ & \text{order } 1, 2, \dots, \text{ or } n_w \\ 1, & \text{otherwise.} \end{cases} \quad \square \tag{18}$$

The optimizer  $z$  in (15) is the diagonal of  $B_a$ . To represent the dependence of the constraint (C5) (in (15)) on  $z$ , the matrix  $B_{cl,i}(z)$  (which is a function of  $B_a$ ) is written as a function of  $z$ . And (18) in Lemma III.7 is a heuristic to convert the decision variables ( $z \in \mathbb{R}^{n_u}$ ) to binary variables.

In this article, to solve the security allocation problem via an SDP, we introduced some approximations. Next, we

provide some discussions on the optimality of the solution obtained via these approximations.

**Theorem III.8.** *Let us represent the optimal solution obtained from (15) as  $\underline{z}$ , the value of (15) as  $\underline{\gamma}$ , the value of (12) as  $\gamma^*$  (albeit unknown), the approximate solution obtained from (18) as  $\bar{B}_a$ . Then the following statements are true.*

- (a) (No loss of optimality) *If  $\text{rank}(\bar{Z}) = 1$ , then  $\bar{B}_a$  is an optimal solution to (12).*
- (b) (When sub-optimal, characterizing a posteriori bound for the optimal risk  $\gamma^*$ ) *Let*

$$\bar{\gamma} \triangleq \inf_v \left\{ v + \frac{1}{1-\alpha} \frac{1}{N} \sum_{i=1}^N [\tilde{q}(\bar{B}_a, \delta_i) - v]^+ \right\}$$

where the value of  $\tilde{q}(\bar{B}_a, \delta_i)$  is computed using the SDP (11). Here  $\bar{\gamma}$  is the CVaR under the sub-optimal attack matrix  $\bar{B}_a$ . Then, it holds that  $\underline{\gamma} \leq \gamma^* \leq \bar{\gamma}$ .

- (c) (When sub-optimal, characterizing a posteriori upper bound for the optimality gap) *Let us define the optimality gap as the difference between the true CVaR  $\bar{\gamma}$ , and the optimal CVaR  $\gamma^*$ . Then it holds that*

$$|\bar{\gamma} - \gamma^*| \leq |\bar{\gamma} - \underline{\gamma}|. \quad \square$$

Theorem III.8 states that the value of the optimal risk ( $\gamma^*$ ) albeit unknown is bounded above and below by known values. It also provides an upper bound on the difference between the true risk ( $\bar{\gamma}$ ) and the optimal risk ( $\gamma^*$ ). In the next section, we discuss the solution to the allocation problem under different risk metrics.

**Remark 5** (Actual risk incurred). *Let  $\zeta = \inf_v v + \frac{1}{1-\alpha} \frac{1}{N} \sum_{i=1}^N [q(\bar{B}_a, \delta_i) - v]^+$  where the value of  $q(\cdot, \cdot)$  is determined from (10). Then the risk incurred by implementing the attack matrix  $\bar{B}_a$  is  $\zeta$ .  $\triangleleft$*

#### IV. Alternative risk measures

The previous section focussed on providing an (approximate) solution to the allocation problem (8) which considered the risk metric CVaR. For the sake of comparison, we briefly study the allocation problem using two other measures of risk (i) Worst case measure, and (ii) nominal measure.

##### A. Worst-case measure

For any random variable  $X(\cdot, \delta)$ ,  $\delta \in \Omega$ , the worst case measure is defined as  $\sup_{\delta \in \Omega} X(\cdot, \delta)$ : which represents the maximum loss that can occur. Then, under the worst-case measure, the allocation problem formulated in (6) becomes

$$\arg \inf_{B_a} \left\{ \sup_{\delta \in \Omega} \{q(B_a, \delta)\} \middle| (C1), (C2) \right\}$$

Similar to approximations in Section III, we first replace  $q(\cdot)$  with  $\tilde{q}(\cdot)$  to make the problem convex. Then we replace  $\Omega$  with the sampled set. Then the design problem becomes

$$\arg \inf_{B_a} \left\{ \sup_{\delta_i, i \in \Omega_N} \{\tilde{q}(B_a, \delta_i)\} \middle| (C1), (C2) \right\}. \quad (19)$$

Next, we propose an approximate solution to (19) in Lemma IV.1 using similar methods adopted in Lemma III.7.

**Lemma IV.1.** *Let  $z \in \mathbb{R}^{n_u}$ . Let  $z^*$  represent the optimal argument of  $z$  from the SDP (20).*

$$\begin{aligned} \min_{\mathcal{S}_6} \quad & t \\ \text{s.t.} \quad & t \geq \epsilon_r \gamma_{1,i} + \epsilon_a \gamma_{2,i}, \quad \forall i \in \Omega_N \\ & (C5), (C8) - (C11) \end{aligned} \quad (20)$$

where  $\mathcal{S}_6 = \{z, t\} \cup \{\cup_{i=1}^N \{X_i, \gamma_{1,i}, \gamma_{2,i}\}\}$ ,  $B_a = \text{diag}(z)$ , and  $Z = \text{diag}(z)$ . Then an approximate binary solution to (19) is given by (18). ■

##### B. Nominal measure

Although we use risk measures for allocation in uncertain systems, it is logical to ask the question: “Is considering risk metrics necessary?”. To answer this question, we outline the allocation strategy when uncertainties are not considered. In other words, we allocate the security measures for the nominal system:  $\inf_{B_a} \{q(B_a, \emptyset) \middle| (C1), (C2)\}$ . Then, similar to (19), we relax the allocation problem as

$$\inf_{B_a} \left\{ \tilde{q}(B_a, \emptyset) \middle| (C1), (C2) \right\}. \quad (21)$$

Next, we propose an approximate solution to (21) by a similar method adopted in Lemma IV.2 whose proof is omitted since it is similar to the proof of Lemma IV.1.

**Lemma IV.2.** *Let  $A_{cl}$ , and  $B_{cl}$  denote the nominal system matrices of (4). And let  $z \in \mathbb{R}^{n_u}$ . Let us represent the optimal*

*argument of  $z$  from the SDP (22) as  $z^*$ .*

$$\begin{aligned} \min_{\mathcal{S}_7} \quad & \epsilon_r \gamma_1 + \epsilon_a \gamma_2 \\ \text{s.t.} \quad & \begin{bmatrix} -I & 0 & C_p X & 0 \\ 0 & -\gamma_1 I & I & 0 \\ X C_p^T & I & \mathcal{W}_2 & B_{cl}(z) \\ 0 & 0 & B_{cl}(z)^T & -\gamma_2 I \end{bmatrix} \preceq 0 \\ & \mathcal{W}_2 = X A_{cl}^T + A_{cl} X - X U^T - U X \\ & (C10), (C11), \\ & \mathcal{S}_7 = \{z, X \succ 0, \gamma_1 \geq 0, \gamma_2 \geq 0\}. \end{aligned} \quad (22)$$

where  $B_a = \text{diag}(z)$ , and  $Z = \text{diag}(z)$ . Then an approximate binary solution to (21) is given by (18). ■

In this section, we outlined the solution to the allocation problem under two other risk metrics. However, in the method that we propose to solve the allocation problem (in Lemma III.7, Lemma IV.1, and Lemma IV.2), there are two sources of suboptimality. The first is the convex relaxation in formulating the convex upper bound  $\tilde{q}(\cdot)$ , and the second while relaxing the non-convex binary constraint (C2).

In the next section, we present two algorithms: an algorithm that is computationally intensive but strictly optimal (exhaustive search), and a greedy algorithm that is polynomial in time but without any optimality guarantees. We also discuss the (de)merits of all three methods.

#### V. Alternative search algorithms

In this section, we outline a method to determine the optimal solution of (8). Before this, we introduce the following notations. The set of all actuators is represented by  $\mathcal{A}$ , and for any finite set  $\mathcal{Q}$ , an element of  $\mathcal{Q}$  is represented by  $q$ .

##### A. Exhaustive search

The exhaustive search algorithm first determines all possible subsets of  $\mathcal{A}$  with maximum cardinality  $n_w$ . Then, it determines the CVaR when these various subsets of actuators are protected. Then the optimal solution to the allocation problem is the set of actuators that yields the minimum CVaR. We outline an exhaustive search in Algorithm 1, where  $g^*$  represents the optimal set of protected actuators.

In Algorithm 1, if the CVaR is determined using  $q(\cdot, \delta_i)$  in (10), the result of the algorithm is optimal. The result of Algorithm 1 can then be then used to compare how the approximation in formulating  $\tilde{q}$  affects the solutions in (15). However, if the CVaR is determined using  $\tilde{q}(\cdot, \delta_i)$  in (11), the algorithm is sub-optimal.

The time complexity of the exhaustive search is very high since the algorithm searches over all possible choices of actuators. Next, we discuss a greedy algorithm that is polynomial in time but provides a sub-optimal solution.

##### B. Greedy search

The greedy algorithm first chooses one actuator to be protected which minimizes the CVaR. Let this actuator be the first actuator  $a_1$ . Now with  $a_1$  being protected, the algorithm searches for one more actuator to be protected such that

**Algorithm 1:** Exhaustive search to solve (8)

**Initialization:**  $\alpha, \Omega_N, \mathcal{A}, n_w$  and an empty list  $\gamma$   
**Step 1:** Determine  $\mathcal{G}$  as the set of all subsets of  $\mathcal{A}$  with cardinality  $n_w$ .  
**Step 2:**  
**forall**  $g \in \mathcal{G}$  **do**  
    Set  $B_a(i, i) = 0$  if  $i \in g$  and 1 otherwise.  
    Determine the  $\text{CVaR}_\alpha\{q(B_a, \delta)\}$  (16) with this new  $B_a$ .  
    Append  $\{\text{CVaR}_\alpha\{q(B_a, \delta)\}, g\}$  to the list  $\gamma$   
**end**  
**Step 3** Determine  $\gamma^* = \min_j \text{CVaR}_\alpha^{[j]}\{q(B_a, \delta)\}$  and the respective  $g^* = g^{[j^*]}$   
**Result:**  $g^*$  ◀

the actuator pair  $\{a_1\} \cup \{a_l\}, l \in \{2, \dots, n_a\}$  minimizes the CVaR. Let this actuator pair be  $\{a_1, a_6\}$ . In this way, the greedy algorithm continues searching for one actuator to protect at a time which minimizes the CVaR until the number of protected actuators is  $n_w$ . This greedy algorithm is depicted in Algorithm 2.

**Algorithm 2:** Greedy search to solve (8)

**Initialization:**  $\alpha, \Omega_N, \mathcal{A}, n_w$ , and empty lists  $\gamma, \mathcal{W}$   
**for**  $j = 1 : n_w$  **do**  
    Clear the list  $\gamma$   
    **for**  $i = 1 : n_u$  **do**  
        Set  $B_a(s, s) = \begin{cases} 0, & \text{if } s \in \mathcal{W}, \text{ or } s = i \\ 1, & \text{otherwise.} \end{cases}$   
        Determine the  $\text{CVaR}_\alpha \tilde{q}(B_a, \delta)$  (16) using the new  $B_a$ .  
        Append  $\gamma$  with  $\text{CVaR}_\alpha \tilde{q}(B_a, \delta)$   
    **end**  
    Determine  $\gamma^* = \min_{k=\{1,2,\dots,n_u\}} \gamma^{[k]}$  and the respective  $k^*$   
    Append  $k^*$  to  $\mathcal{W}$ .  
**end**  
**Result:**  $\mathcal{W}$  ◀

In Algorithm 2, the result  $\mathcal{W}$  represents the sub-optimal set of actuators to be protected. The result is suboptimal since the algorithm does not search over all sets of possible actuators. The greedy algorithm is included in this article for comparison of performance. Also, if the submodularity and non-increasing property of  $\text{CVaR}(q(\cdot))$  is proven, then the greedy algorithm can give certain performance guarantees [44]: which is left for future work.

So far, we discussed three methods to (approximately) solve (8). Our proposed SDP method (15) is an approximate solution and has polynomial time complexity in the worst case. The exhaustive search in Algorithm 1 provides the optimal solution but has combinatorial complexity. Finally, the greedy algorithm is also polynomial in time complexity

but provides a sub-optimal solution. However, as mentioned before, the greedy algorithm has some scope for future work. Next, we compare the methods through a numerical example.

**Remark 6.** *The exhaustive and greedy search algorithms can also be used with other risk metrics. For instance, instead of CVaR, we can determine the worst case or the nominal measure of  $\tilde{q}(\cdot)$  in Algorithm 1 and Algorithm 2. However, we do not detail this due to lack of space.* ◀

## VI. Numerical example

The effectiveness of the method discussed in Lemmas III.7 is illustrated through numerical examples in this section. Consider the system in (1)-(3) with matrices given in (7) and  $B = B_a = I_4$ . We set  $\epsilon_r = 1, \epsilon_a = 300$ , and  $N = 500$ . We sample  $\Omega$  according to sample distribution. Then, we determine the value of  $q(B_a, \delta_i)$  using (10) and  $\tilde{q}(B_a, \delta_i)$  using (11) which are plotted in Figure 3.

In line with Remark 2, the value of  $q(\cdot, \delta)$  is bounded for all uncertainties  $\delta \in \Omega$ . To recall, the value of  $q(\cdot, \delta)$  (attack impact) is bounded since the attack energy is bounded. Also, in line with Lemma III.4,  $q(\cdot)$  is upper bounded by  $\tilde{q}(\cdot)$ .

The rest of this section is organized as follows. In Section VI.A, we compare the metric (10) to other security metrics in the literature. In Section VI.B we compare the results to the allocation problem when using CVaR and the nominal measure, whereas in Section VI.C we compare CVaR against the worst-case measure. In section VI.D, we compare the different search algorithms. Finally, in Section VI.E, we compare the solution from (15) to the optimal solution.

### A. Comparison with other metrics

Following the discussion in section II.E, to compare our metric (5) to other security metrics, we proceed as follows. We set  $B^T = [1 \ 0 \ 0 \ 0]$ , and  $B_a = 1$ . Then we determine the value of  $q(\cdot, \emptyset)$  by solving (10) (equivalent to (5)) when  $\epsilon_a = 10^6$  and  $\epsilon_r = 1$ . This makes the constraint on the attack energy inactive making  $q(\cdot)$  the OOG. We found this value to be 34.45. Next, we determine the true OOG by solving [4, (6.18)] and these values match.

We set  $\epsilon_r = 10^6$  and  $\epsilon_a = 1$ . This makes the constraint on the detection output inactive, making  $q(\cdot)$  the  $H_\infty$  metric. We found the value of  $q(\cdot)$  to be 0.62. We also determine the value of the  $H_\infty$  metric by solving the LMI in [38] and these values match. Thus we numerically depict the relation between (5) and other metrics.

### B. Comparison with nominal measure.

Next we set  $N = 100, \alpha = 0.8, \epsilon_r = 1$ , and  $\epsilon_a = 300$ . For the sake of comparison, we determine the  $\text{CVaR}_{0.8}(\tilde{q}(\cdot))$  when  $n_w = 0$  (no protection) as 2813.6. Next, we allocate the security measure that minimizes  $\text{CVaR}_{0.8}(\tilde{q}(\cdot))$  by solving the optimization problem (15) and obtain the actuators to be protected as  $A_2$  and  $A_4$  (here  $A_i, i \in \{1, \dots, n_u\}$  represents the  $i^{\text{th}}$  actuator).

To depict the effectiveness of using a risk metric, we solve the allocation problem which minimizes  $\tilde{q}(\cdot, \emptyset)$ , i.e.,

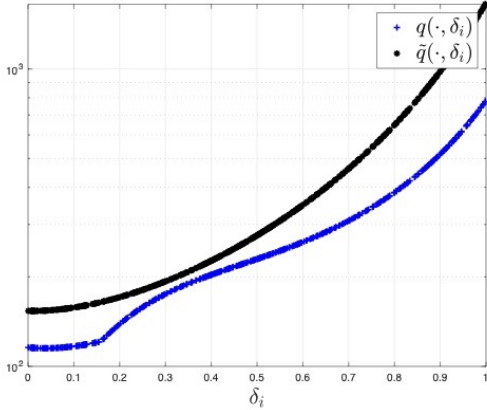


**FIGURE 3.** The values of  $q(B_\alpha = I_4, \delta_i)$  and  $\tilde{q}(B_\alpha = I_4, \delta_i)$  across different  $\delta_i$ , obtained by solving (10) and (11) respectively.

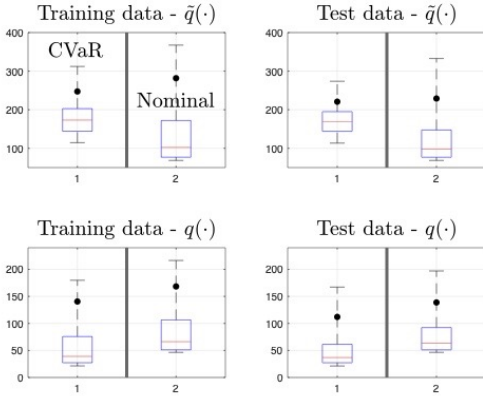


**FIGURE 4.** The box plots with  $N = 100$  in the top (bottom) depicts the value of the attack impact  $q(\cdot)$  (the impact proxy  $\tilde{q}(\cdot)$ ) when the protected actuators are obtained from optimizing the CVaR ( $A_2$  and  $A_4$ ) in (15) and the nominal measure ( $A_1$  and  $A_4$ ) in (22). The plots on the left (right) represent values obtained from training (test) data. Here training data represents the data points (of uncertainty) used in the optimization problem, and test data represents new data points (of uncertainty). On each box, the central mark indicates the median, and the bottom and top edges of the box indicate the 25<sup>th</sup> and 75<sup>th</sup> percentiles, respectively, and the black dot represents the  $\text{CVaR}_{0.8}$  of the data points. The whiskers extend to the most extreme data points.

using the nominal measure, by solving (22). We obtain the actuators to be protected as  $\{A_1, A_4\}$ .

To visualize the effectiveness of the used metric, in Fig 4, we plot the value of the attack impact  $q(\cdot)$ , the impact proxy  $\tilde{q}(\cdot)$  when the protected actuators are  $\{A_2, A_4\}$ , and  $\{A_1, A_4\}$  respectively. Now some remarks are in order.

Firstly, as expected, we see that using the risk metric instead of the nominal measure reduces the CVaR (the black dots in Figure 4) across training and test data, and across  $q(\cdot)$  and  $\tilde{q}(\cdot)$ . Secondly, using a risk metric minimizes the worst-case impact and the impact proxy (the top whiskers of the box plots in Fig 4). Thirdly, although the median of the impact proxy (the red horizontal lines in Figure 4) is higher when using the risk metric, the median of the actual impact

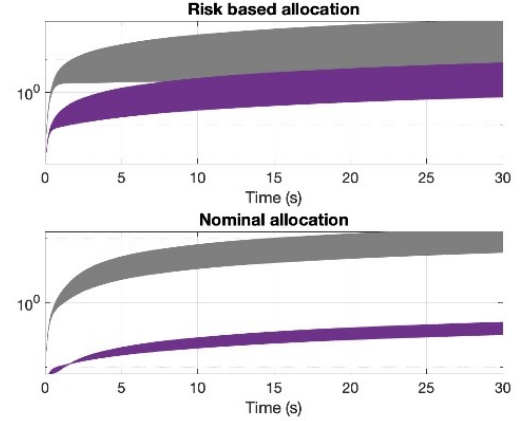


**FIGURE 5.** Performance energy (grey) and detection energy (violet) for  $N = 500$  different realizations of uncertainty, under CVaR-based allocation strategy (top), and the nominal allocation strategy (bottom).

$q(\cdot)$  is lower. Finally, we see that the 25<sup>th</sup> percentile of the impact  $q(\cdot)$  is lower when using the risk metric.

Next we consider a step attack signal  $a(t) = \mathbf{1}$ ,  $t \geq 0$ . Under the step attack, the performance energies under  $N = 500$  different realizations of the uncertainty are shown in Figure 5. The performance energy when the allocation is done by optimizing the CVaR is depicted at the top of Figure 5, and the nominal measure is depicted at the bottom of Figure 5. As mentioned before, the objective of the allocation problem is to minimize the performance loss under attacks. From Figure 5 we see that the worst-case performance loss is the same (approximately) under the different allocation strategies. However, under the CVaR-based allocation, the best-case performance loss is low, thus depicting an advantage.

The detection energies are depicted in violet colour in Figure 5. As mentioned before, the objective of the allocation problem is to maximize the detection output energy and raise an alarm when  $\|y_r\|_{\ell_2}^2 > \epsilon_r$ . When  $\epsilon_r = 1$ , under the nominal allocation strategy, we can see from Figure 5 that the alarm will never be raised, thus depicting a poor performance. In other words, for attack detection,  $\epsilon_r$  should be as low as 0.1 which can be impractical in the presence of noise. However, under the CVaR-based allocation strategy, the attack is detected when  $\epsilon_r = 1$ . Thus, our method can help to detect attacks better. The high performance deterioration under attack may be prevented by timely switching to a fault-tolerant controller when the attack is detected.

### C. Comparison with worst-case measure.

For this comparison, we now consider a distributed NCS, consisting of agents with single integrator dynamics as described in [20]. The operator is uncertain about the edge weights of the undirected graph. Each agent has a wireless control loop that is prone to attack. The system matrices of

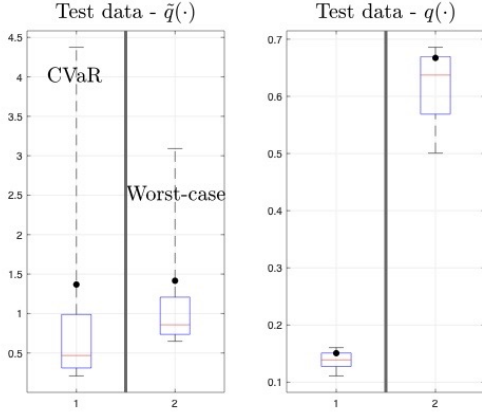


**FIGURE 6.** The box plots with  $N = 500$  in the left (right) depicts the value of the impact proxy  $\tilde{q}(\cdot)$  (attack impact  $q(\cdot)$ ) when the protected actuators are obtained from optimizing the CVaR  $(\{A_1, A_2, A_3\})$  in (15) and the worst-case  $(\{A_1, A_2, A_6\})$  in (20). On each box, the black dot represents the CVaR $_{0.5}$  of the data points.

the NCS (derived similar to [20, (6)]) are  $A_{cl}^\Delta =$

$$A_{cl}^\Delta = \begin{bmatrix} \delta - 32 & 4 & 0 & 3 & 0 & 5 + \delta \\ 4 & -37 & 3 & 4 & 4 & 0 \\ 0 & 3 & -29 & 2 & 0 & 0 \\ 3 & 4 & 2 & -33 & 3 & 0 \\ 0 & 4 & 0 & 3 & -28 & 1 \\ 5 + \delta & 0 & 0 & 0 & 1 & \delta - 24 \end{bmatrix} \quad (23)$$

where  $\delta \in \Omega \triangleq [-1, 0]$ ,  $B_{cl} = I_6$ , and  $\begin{bmatrix} C_p \\ C_r \end{bmatrix} \triangleq \begin{bmatrix} 0 & 0 & 1 & 0 & 0 & 0 \\ 0 & 0 & 0 & 0 & 0 & 1 \end{bmatrix}$ . Here  $\delta$  represents the uncertainty in the edge weights of the NCS. We set  $N = 1000$ ,  $n_w = 3$ ,  $\alpha = 0.5$ . We are now interested in allocating the security measure which minimizes the CVaR $_{0.5}(\tilde{q}(\cdot))$ . To this end, we solve the optimization problem (15) and obtain the actuators to be protected as  $\{A_1, A_2, A_3\}$ . For comparison, we solve the allocation problem that minimizes the worst-case impact (20), and we obtain the actuators to be protected as  $\{A_1, A_2, A_6\}$ . To visualize the effectiveness of the used metric, in Fig 6, we plot the values of the attack impact  $q(\cdot)$  and the impact proxy  $\tilde{q}(\cdot)$  for some test data when protected actuators are  $\{A_1, A_2, A_3\}$ , and  $\{A_1, A_2, A_6\}$ , respectively.

Firstly, as expected, we see that using CVaR as a risk metric reduces the CVaR of  $\tilde{q}(\cdot)$  (black dot in Figure 6). Secondly, using CVaR causes the worst-case impact (top whiskers of  $q$ ) to be low. Finally, using the CVaR as a risk metric reduces the median (red horizontal line in the box plot), and the 25<sup>th</sup> percentile across  $q(\cdot)$  and  $\tilde{q}(\cdot)$ .

#### D. Comparison with other search algorithms

Now we have shown the effectiveness of using CVaR as a risk metric. Next, we show the effectiveness of the proposed allocation method. To this end, we first solve the allocation problem through an exhaustive search. That is, we consider the system matrices in (23) and solve the allocation problem

Method	$N = 100$	$N = 200$
SDP (15)	3.77 sec	7.77 sec
Algorithm 1 (Exhaustive search)	262.30 sec	523.29 sec
Algorithm 2 (Greedy search)	243.26 sec	469.19 sec

**TABLE 1.** Comparison of results

which minimizes the CVaR $_{0.3}$  by an exhaustive search as in Algorithm 1. Similarly, we also solve the problem using greedy search in Algorithm 2. We observe that the results are the same as obtained by using our SDP (15): that is, we obtain that the protected actuators are  $\{A_1, A_2, A_3\}$ . However, the time taken to obtain these results are significantly different and are given in TABLE 1. The results are tabulated when  $N = 100$  and  $N = 200$ . We can see that the computational time for the convex SDP that we propose in this article is at least 40 times faster than the other two methods, thereby depicting its efficacy.

#### E. Comparison to the optimal solution

Next, we discuss the loss of optimality in the proposed SDP (15) due to the approximation in formulating  $\tilde{q}$ . We compare the solution obtained from (15) to the solution obtained from Algorithm 1 when  $q(\cdot)$  from (10) is used to determine the CVaR. Recall that when  $q(\cdot)$  from (10) is used in Algorithm 1, it provides the optimal solution.

As we already know, the solution from (15) is  $\{A_1, A_2, A_3\}$ . We obtain the optimal solution from Algorithm 1 to be  $\{A_2, A_3, A_6\}$  when  $q(\cdot)$  is used. Thus, we can see that there is a loss of optimality here. However, we report that the difference in the CVaR between these two solutions in the test data is only 0.02 which is negligible.

## VII. Conclusions

This article considered the problem of security measure allocation when the actuators of an uncertain NCS are under attack. The CVaR was used to formulate the risk associated with the attack impact. The allocation problem was observed to be hard to solve since it involves SDP constraints with binary decision variables. Thus we use Young's relation to formulate a relaxed convex SDP. We also briefly compare our algorithm across different risk metrics and different search algorithms: discussing its merits and demerits. The efficacy of our proposed approach is discussed through numerical examples. Future works include providing any performance guarantees on the proposed approach.

## Appendix

### A.1. Proof of Lemma III.1

*Proof:*

Consider the constraint  $\|a_i\|_{\mathcal{L}_2}^2 \leq \epsilon_a$  in (5). We know that  $\|a_i\|_{\mathcal{L}_2}^2 \leq \epsilon_a \implies \lim_{t \rightarrow \infty} a_i(t) = 0$ . Since the closed loop system is stable,  $\lim_{t \rightarrow \infty} a_i(t) = 0 \implies \lim_{t \rightarrow \infty} x_i(t) \triangleq x_i(\infty) = 0$ . Then, for a given  $\delta_i$ ,  $q(B_a, \delta_i)$  in (5) can be

reformulated using the hypergraph formulation as (24).

$$\sup_{v, a \in \mathcal{L}_{2e}} \left\{ v \left\{ \begin{array}{l} \|y_{p,i}\|_{\mathcal{L}_2}^2 \geq v \\ \|a_i\|_{\mathcal{L}_2}^2 \leq \epsilon_a \end{array} \right. \right. \left. \left. \begin{array}{l} \|y_{r,i}\|_{\mathcal{L}_2}^2 \leq \epsilon_r \\ x_i(\infty) = 0 \end{array} \right\} \right\} \quad (24)$$

Note that (24) is similar to [34, (22)]. Then, following the proof of [34, Theorem 4.4], (24) can be rewritten as [34, (51)] which concludes the proof. ■

## A.2. Proof of Lemma III.2

Before we present the proof, we present an intermediate result which helps in constructing the proof of Lemma III.2.

**Proposition A.2.1** ([35]). *Consider a CT system  $\Sigma \triangleq (A, B, C, D)$  which is controllable and observable with supply rate  $s[\cdot] = \|y_1(t)\|_2^2 - \|y_2(t)\|_2^2 + \|u(t)\|_2^2$ . Let  $y_i(t) = C_i x(t) + D_i u(t)$ ,  $i = \{1, 2\}$ . Then the following statements are equivalent:*

- 1) For all trajectories of the system, for  $T > 0$  and  $x[0] = 0$ , we have  $\int_0^T s[x(t), u(t)] dt \geq 0$ .
- 2) There exists a symmetric  $P \succeq 0$  such that (25) holds.

$$\begin{bmatrix} A^T + PA & PB \\ B^T P & 0 \end{bmatrix} + R \preceq 0, \quad (25)$$

$$R \triangleq \begin{bmatrix} C_1^T \\ D_1^T \end{bmatrix} \begin{bmatrix} C_1 & D_1 \end{bmatrix} - \begin{bmatrix} C_2^T \\ D_2^T \end{bmatrix} \begin{bmatrix} C_2 & D_2 \end{bmatrix} - \begin{bmatrix} 0 & 0 \\ 0 & I \end{bmatrix} \square$$

**Remark A.2.1** ([45]). *Suppose that (i)  $\Sigma$  is minimal, and (ii) for all  $0 \neq y = [y_1^T y_2^T]^T$ ,  $\exists u$  such that  $s[\cdot] < 0$ , then  $\Sigma$  is dissipative iff  $\exists P \succ 0$  such that (25) holds.* ◁

Next, we present the proof of Lemma III.2.

*Proof:*

Let us define a (supply rate) function  $s[\cdot] \triangleq -\|y_p(t)\|_{\mathcal{L}_2}^2 + \gamma_1 \|y_r(t)\|_{\mathcal{L}_2}^2 + \gamma_2 \|a(t)\|_{\mathcal{L}_2}^2$  which is also the constraint of the optimization problem (9). Recall that the signals  $(y_p, y_r, u)$  obey the condition of Proposition A.2.1: they originate from a system that is controllable and observable (Assumption II.2). Then using (25), the constraint of (9) can be replaced by (10). It only remains to show that  $P \succ 0$ .

It holds that  $P \succ 0$  if the conditions of Remark A.2.1 hold which we show next. Condition (i) holds from Assumption II.2. And for any non-zero  $y$ ,  $\gamma_2$  in  $s[\cdot]$  can be increased arbitrarily such that  $s[\cdot] < 0$ . Thus, the conditions of Remark A.2.1 hold which concludes the proof. ■

## A.3. Proof of Theorem III.3

*Proof:*

Applying Schur complement,  $(C3_i)$  in (10) becomes

$$\mathcal{W}_3 \triangleq \begin{bmatrix} -I & C_p & 0 \\ C_p^T & A_{cl,i}^T P_i + P_i A_{cl,i} - \gamma_{1,i} U^T U & P_i B_{cl,i} \\ 0 & B_{cl,i}^T P_i & -\gamma_{2,i} I \end{bmatrix} \preceq 0$$

We now apply congruence transformation [46, Section 2.2] which states that the matrix inequality  $\mathcal{W}_3 \preceq 0$  is satisfied if

and only if  $Z \mathcal{W}_3 Z^T \preceq 0$  where  $\text{rank}(Z) = n$ . We pick  $Z = \text{diag}(I, P_i^{-1}, I)$ . Then the first constraint of (10) becomes

$$\begin{bmatrix} -I & C_p X_i & 0 \\ X_i C_p^T & X_i A_{cl,i}^T + A_{cl,i} X_i - \mathcal{W}_4 & B_{cl,i} \\ 0 & B_{cl,i}^T & -\gamma_{2,i} I \end{bmatrix} \preceq 0 \quad (26)$$

where  $\mathcal{W}_4 \triangleq \gamma_{1,i} X_i U^T U X_i$  and  $X_i = P_i^{-1}$ . Up to now, we have shown that (10) (or equivalently (26)) is convex in  $B_a$  (since  $B_{cl,i}$  is linear in  $B_a$ ) except  $\mathcal{W}_4$ . We next approximate

$$\mathcal{W}_4 \succeq_1 U X_i + X_i U - \gamma_{1,i}^{-1} I \triangleq \tilde{\mathcal{W}}_4, \quad (27)$$

where the inequality 1 is from Young relation which is given by  $\gamma^{-1} G^T G \succeq G + G^T \gamma I$  for any given matrix  $G$  and  $\gamma \geq 0$  [46, Section 2.4.3]. We now relax the constraint (26) by replacing  $\mathcal{W}_4$  by  $\tilde{\mathcal{W}}_4$ . Then taking the Schur complement of the relaxed constraint concludes the proof. ■

## A.4. Proof of Lemma III.4

*Proof:*

The optimal tuple for (11) is represented by  $(\bar{X}_i, \bar{\gamma}_{1,i}, \bar{\gamma}_{2,i})$ , by applying Schur complement to its first constraint, we get

$$Q + \begin{bmatrix} -\bar{X}_i U - U \bar{X}_i + \gamma_{1,i}^{-1} I & 0 \\ 0 & 0 \end{bmatrix} \preceq 0. \quad (28)$$

where  $Q \triangleq \begin{bmatrix} \bar{X}_i A_{cl,i}^T + A_{cl,i} \bar{X}_i + \bar{X}_i C_p^T C_p \bar{X}_i & B \\ B^T & -\gamma_{2,i} I \end{bmatrix}$ . Then by using (27), (28) becomes

$$Q + \begin{bmatrix} \gamma_{1,i} \bar{X}_i U^T U \bar{X}_i & 0 \\ 0 & 0 \end{bmatrix} \preceq 0 \quad (29)$$

We apply congruence transformation with  $Z = \text{diag}(\bar{P}_i, I)$ . Then (29) is equivalent to

$$\begin{bmatrix} A_{cl,i} \bar{P}_i + \bar{P}_i A_{cl,i} + C_p^T C_p - \gamma_{1,i} C_r^T C_r & \bar{P}_i B_{cl} \\ B_{cl,i}^T \bar{P}_i & -\gamma_{2,i} I \end{bmatrix} \preceq 0$$

which is the constraint of (10). This concludes the first part of the proof. We prove the second proof by contradiction. For a given uncertainty  $\delta_i$ , let the optimal tuple of (11) be  $(\cdot, \gamma_{1R}, \gamma_{2R})$ . Similarly, let the optimal tuple of (10) be  $(\cdot, \gamma_{1O}, \gamma_{2O})$ . Let us assume that  $\gamma_R = \epsilon_1 \gamma_{1R} + \epsilon_2 \gamma_{2R} < \epsilon_1 \gamma_{1O} + \epsilon_2 \gamma_{2O} = \gamma_O$ . We know from Theorem III.4 that every feasible tuple of (11) is a feasible tuple of (10). Then  $\gamma_{1R}, \gamma_{2R}$  is a feasible solution to (10) which yields a lower value to (10). However, this contradicts the assumption and concludes the proof. ■

## A.5. Proof of Lemma III.5

*Proof:*

Let  $z$  be the diagonal elements of  $B_a$  (recall that only the diagonal elements of  $B_a$  are the design variables). Now we show that when the constraints of (13) are satisfied, the variable  $z$  is binary. Using Schur complement,  $(C10)$  can be rewritten as  $Z - z z^T \succeq 0$ . And since the  $\text{rank}(Z) = 1$ , we can conclude  $\mathcal{Z} \triangleq Z - z z^T = 0$ . Let us consider the diagonal elements of the matrix  $\mathcal{Z}$ , which yields  $z_i(1 - z_i) = 0$  whose solutions are  $z_i = \{0, 1\}$ . This concludes the proof. ■

## A.6. Proof of Lemma III.7

*Proof:*

Consider the objective function in (17). Given  $\delta_i$ , let  $\tilde{q}(B_a, \delta_i) - v \triangleq t_i$ . Then the projection of  $t_i$  on the positive real axis is achieved by the constraints (C6) and (C7). Then the value of  $\tilde{q}(B_a, \delta_i)$  is given by solving the optimization problem (11). Thus  $\tilde{q}(B_a, \delta_i)$  is replaced by the objective function of (11) and the corresponding constraint (C5) is included. The constraint (C1) is re-written as (C11). Using Lemma III.5 (C2) is relaxed as (C10). The optimal argument  $z^*$  of (15) will not be binary but integers. To this end, let  $\mathcal{K}$  denote a set that contains the  $n_w$  least elements in the value of  $z^*$ . Then, the actuator channel  $i$  is protected if  $z_i$  belongs  $\mathcal{K}$ . This concludes the proof. ■

## A.7. Proof of Theorem III.8

*Proof of (a):* The optimization problem (15) was formulated by removing the rank constraint  $\text{rank}(Z) = 1$  from (13). However, if the rank constraint is satisfied implicitly, the solution  $\bar{B}_a$  is optimal. This concludes the proof of (a).

*Proof of (b):* Let us consider the optimization problem (12) whose value is  $\gamma^*$ . The value of  $\gamma^*$  is the same as the value of (13) since they are equivalent. In the optimization problem (15), we removed the rank constraint. Since (15) is a minimization problem, its value will be lower than (13). Thus it holds that  $\underline{\gamma} \leq \gamma^*$ . Since the approximate solution  $\bar{B}_a$  obtained from (18) is sub-optimal, but feasible to the optimization problem (12), the corresponding risk:  $\bar{\gamma} = \text{CVaR}_\alpha(\tilde{q}(\bar{B}_a, \cdot))$  will be higher than the true risk. Thus  $\bar{\gamma}$  acts as an upper bound for the true risk  $\gamma^*$ . Then, the following holds  $\gamma^* \leq \bar{\gamma}$ . Combining the above two arguments concludes the proof of (b).

*Proof of (c):* The proof follows directly from (b), and the fact that the quantities  $(\bar{\gamma} - \gamma^*)$  and  $\bar{\gamma} - \underline{\gamma}$  are positive. This concludes the proof. ■

## A.8. Proof of Lemma IV.1

*Proof:*

Using the hyper-graph formulation, and the SDP (11), the objective function in (19):  $\sup \tilde{q}(\cdot)$ , can be re-written as  $t \geq \epsilon_r \gamma_{1,i} + \epsilon_a \gamma_{2,i}, \forall i \in \Omega_N$ . The corresponding constraint (C4) is included. The constraint (C1) is re-written as (C11). And an SDP relaxation of the constraint (C2) is formulated using (C10). The optimal argument  $z^*$  of (15) will not be binary but integers. To this end, let  $\mathcal{K}$  denote a set that contains the  $n_w$  least elements in the value of  $z^*$ . Then, actuator  $i$  is protected if  $z_i$  belongs  $\mathcal{K}$ . This concludes the proof. ■

## REFERENCES

- [1] H. Sandberg, V. Gupta, and K. H. Johansson, "Secure networked control systems," *Annual Review of Control, Robotics, and Autonomous Systems*, vol. 5, pp. 445–464, 2022.
- [2] S. M. Dibaji, M. Pirani, D. B. Flamholz, A. M. Annaswamy, K. H. Johansson, and A. Chakraborty, "A systems and control perspective of cps security," *Annual reviews in control*, vol. 47, pp. 394–411, 2019.
- [3] M. S. Chong, H. Sandberg, and A. M. Teixeira, "A tutorial introduction to security and privacy for cyber-physical systems," in *2019 18th European Control Conference (ECC)*, pp. 968–978, IEEE, 2019.
- [4] R. M. Ferrari and A. M. Teixeira, *Safety, Security and Privacy for Cyber-Physical Systems*. Springer, 2021.
- [5] J. Giraldo, D. Urbina, A. Cardenas, J. Valente, M. Faisal, J. Ruths, N. O. Tippenhauer, H. Sandberg, and R. Candell, "A survey of physics-based attack detection in cyber-physical systems," *ACM Computing Surveys (CSUR)*, vol. 51, no. 4, pp. 1–36, 2018.
- [6] J. Li, Z. Wang, Y. Shen, and L. Xie, "Attack detection for cyber-physical systems: A zonotopic approach," *IEEE Transactions on Automatic Control*, 2023.
- [7] N. Hashemi and J. Ruths, "Co-design for resilience and performance," *IEEE Transactions on Control of Network Systems*, pp. 1–12, 2022.
- [8] J. P. Hespanha and S. D. Bopardikar, "Output-feedback linear quadratic robust control under actuation and deception attacks," in *2019 Am. Control Conference (ACC)*, pp. 489–496, IEEE, 2019.
- [9] F. Fotiadis and K. G. Vamvoudakis, "Concurrent receding horizon control and estimation against stealthy attacks," *IEEE Transactions on Automatic Control*, 2022.
- [10] J. Milošević, A. Teixeira, T. Tanaka, K. H. Johansson, and H. Sandberg, "Security measure allocation for industrial control systems: Exploiting systematic search techniques and submodularity," *International Journal of Robust and Nonlinear Control*, vol. 30, no. 11, pp. 4278–4302, 2020.
- [11] S. Tom, D. Christiansen, and D. Berrett, "Recommended practice for patch management of control systems," tech. rep., Idaho National Lab.(INL), Idaho Falls, ID (United States), 2008.
- [12] S. Beattie, S. Arnold, C. Cowan, P. Wagie, C. Wright, and A. Shostack, "Timing the application of security patches for optimal uptime.," in *LISA*, vol. 2, pp. 233–242, 2002.
- [13] A. Risley, J. Roberts, and P. LaDow, "Electronic security of real-time protection and SCADA communications," *Schweitzer Engineering Laboratories, SEL*, 2003.
- [14] M. Ekstedt, *Operator authentication and accountability for SCADA servers when requests are forwarded by a middle layer*. PhD thesis, Aalto University, 2018.
- [15] M. Hadley and K. Huston, "Secure SCADA communication protocol performance test results," *Pacific Northwest National Laboratory (August 2007)*, 2007.
- [16] Y. Mo and B. Sinopoli, "Secure control against replay attacks," in *2009 47th annual Allerton conference on communication, control, and computing (Allerton)*, pp. 911–918, IEEE, 2009.
- [17] R. M. Ferrari and A. M. Teixeira, "A switching multiplicative watermarking scheme for detection of stealthy cyber-attacks," *IEEE Trans. on Automatic Control*, vol. 66, no. 6, pp. 2558–2573, 2020.
- [18] D. Du, C. Zhang, X. Li, M. Fei, T. Yang, and H. Zhou, "Secure control of networked control systems using dynamic watermarking," *IEEE Trans. on Cybernetics*, vol. 52, no. 12, pp. 13609–13622, 2021.
- [19] G. Dán and H. Sandberg, "Stealth attacks and protection schemes for state estimators in power systems," in *2010 first IEEE International Conference on Smart Grid Communications*, pp. 214–219, IEEE, 2010.
- [20] A. T. Nguyen, S. C. Anand, and A. M. Teixeira, "A zero-sum game framework for optimal sensor placement in uncertain networked control systems under cyber-attacks," in *2022 IEEE 61st Conference on Decision and Control (CDC)*, pp. 6126–6133, IEEE, 2022.
- [21] R. T. Rockafellar and S. Uryasev, "Optimization of conditional value-at-risk," *Journal of risk*, vol. 2, pp. 21–42, 2000.
- [22] A. Krause, A. Roper, and D. Golovin, "Randomized sensing in adversarial environments," in *Twenty-Second International Joint Conference on Artificial Intelligence*, 2011.
- [23] A. Rahmattalabi, P. Vayanos, and M. Tambe, "A robust optimization approach to designing near-optimal strategies for constant-sum monitoring games," in *Decision and Game Theory for Security: 9th International Conference, GameSec 2018, Seattle, WA, USA, October 29–31, 2018, Proceedings 9*, pp. 603–622, Springer, 2018.
- [24] M. Pirani, E. Nekouei, H. Sandberg, and K. H. Johansson, "A game-theoretic framework for security-aware sensor placement problem in networked control systems," *IEEE Transactions on Automatic Control*, vol. 67, no. 7, pp. 3699–3706, 2021.
- [25] M. Pirani, J. A. Taylor, and B. Sinopoli, "Strategic sensor placement on graphs," *Systems & Control Letters*, vol. 148, p. 104855, 2021.

- [26] J. Milošević, M. Dahan, S. Amin, and H. Sandberg, "Strategic monitoring of networked systems with heterogeneous security levels," *arXiv preprint arXiv:2304.04131*, 2023.
- [27] J. Milošević, M. Dahan, S. Amin, and H. Sandberg, "A network monitoring game with heterogeneous component criticality levels," in *2019 IEEE 58th Conference on Decision and Control (CDC)*, pp. 4379–4384, IEEE, 2019.
- [28] S. C. Anand and A. M. Teixeira, "Joint controller and detector design against data injection attacks on actuators," *IFAC-PapersOnLine*, vol. 53, no. 2, pp. 7439–7445, 2020.
- [29] S. C. Anand and A. M. Teixeira, "Risk-averse controller design against data injection attacks on actuators for uncertain control systems," in *2022 Am. Control Conference (ACC)*, pp. 5037–5042, IEEE, 2022.
- [30] S. C. Anand, A. M. Teixeira, and A. Ahlén, "Risk assessment and optimal allocation of security measures under stealthy false data injection attacks," in *2022 IEEE Conference on Control Technology and Applications (CCTA)*, pp. 1347–1353, IEEE, 2022.
- [31] W. Tan, "Unified tuning of pid load frequency controller for power systems via IMC," *IEEE Trans. on power systems*, vol. 25, no. 1, pp. 341–350, 2009.
- [32] M. Verhaegen and V. Verdult, *Filtering and system identification: a least squares approach*. Cambridge university press, 2007.
- [33] T. Gally, M. E. Pfetsch, and S. Ulbrich, "A framework for solving mixed-integer semidefinite programs," *Optimization Methods and Software*, vol. 33, no. 3, pp. 594–632, 2018.
- [34] S. C. Anand, A. M. Teixeira, and A. Ahlén, "Risk assessment of stealthy attacks on uncertain control systems," *arXiv preprint arXiv:2106.07071*, 2021.
- [35] H. L. Trentelman and J. C. Willems, "The dissipation inequality and the algebraic riccati equation," in *The Riccati Equation*, pp. 197–242, Springer, 1991.
- [36] I. R. Petersen, V. A. Ugrinovskii, and A. V. Savkin, *Robust Control Design Using  $H_\infty$  Methods*. Springer Science & Business Media, 2012.
- [37] M. I. Müller, J. Milošević, H. Sandberg, and C. R. Rojas, "A risk-theoretical approach to  $H_2$ -optimal control under covert attacks," in *2018 IEEE Conf on Decision and Contr (CDC)*, pp. 4553–4558, IEEE.
- [38] G. Hilhorst, G. Pipeleers, R. C. Oliveira, P. L. Peres, and J. Swevers, "On extended LMI conditions for  $H_2/H_\infty$  control of DT linear systems," *IFAC Proc. Volumes*, vol. 47, no. 3, pp. 9307–9312, 2014.
- [39] S. D. Bopardikar, A. Speranzon, and J. P. Hespanha, "An  $H_\infty$  approach to stealth-resilient control design," in *2016 Resilience Week (RWS)*, pp. 56–61, IEEE, 2016.
- [40] S. You and N. Matni, "A convex approach to sparse  $H_\infty$  analysis & synthesis," in *2015 54th IEEE Conference on Decision and Control (CDC)*, pp. 6635–6642, IEEE, 2015.
- [41] G. Yuan and B. Ghanem, "Binary optimization via mathematical programming with equilibrium constraints," *arXiv preprint arXiv:1608.04425*, 2016.
- [42] M. Fischetti and A. Lodi, "Heuristics in mixed integer programming," *Wiley encyclopedia of operations research and management science*, 2010.
- [43] M. I. Müller and C. R. Rojas, "Risk-theoretic optimal design of output-feedback controllers via iterative convex relaxations," *Automatica*, vol. 136, p. 110042, 2022.
- [44] L. A. Wolsey, "An analysis of the greedy algorithm for the submodular set covering problem," *Combinatorica*, vol. 2, no. 4, pp. 385–393, 1982.
- [45] G. C. Goodwin and K. S. Sin, *Adaptive filtering prediction and control*. Courier Corporation, 2014.
- [46] R. J. Caverly and J. R. Forbes, "LMI properties and applications in systems, stability, and control theory," *arXiv preprint arXiv:1903.08599*, 2019.